

The high yield is due partly to the high percentage of oxygen in the  $\text{TiO}_2$  targets. It is probably also helped by the rather small barrier seen by the transferring deuteron and by the very large number of states possible in  $\text{F}^{18}$  when the  $Q$  value is 6.1 Mev. By contrast, the  $\text{O}^{16}(\text{Li}^6, n)\text{Na}^{21}$  reaction, where an entire lithium nucleus must pass through the Coulomb barrier, is 17 times smaller.

The 40-sec activity from the  $\text{F}^{19}(\text{Li}^6, 2p)\text{Ne}^{23}$  reaction could be barely detected in the presence of the very large amount of 11-sec  $\text{F}^{20}$  from the  $\text{F}^{19}(\text{Li}^6, \text{Li}^6)\text{F}^{20}$  reaction, Fig. 6. The high yield for the  $\text{F}^{20}$  reaction is undoubtedly due to the ease with which the neutron can tunnel from one nucleus to the other. The  $\text{Ne}^{23}$  reaction probably involves an entirely different mechanism.

In spite of the very high atomic number of the target, the yield of the  $\text{Na}^{23}(\text{Li}^6, \text{Li}^5)\text{Na}^{24}$  reaction, Fig. 6, is about the same as that of  $\text{O}^{16}(\text{Li}^6, n)\text{Na}^{21}$ . As in the  $\text{F}^{20}$  reaction, the neutron encounters a small nuclear barrier, but no Coulomb barrier. There is a larger error in the sodium reaction points than with most of the other reactions. The long, 15-hr half-life of  $\text{Na}^{24}$  required long bombardments which resulted in considerable buildup of  $\text{F}^{18}$  activity from impurities and sometimes in a sputtering away of part of the target. The reaction  $\text{Na}^{23}(\text{Li}^7, \text{Li}^6)\text{Na}^{24}-0.3$  Mev was searched for without success. This sets an upper limit for this reaction of 1.6 atoms of  $\text{Na}^{24}$  for each microcoulomb of 3.5-Mev  $\text{Li}^+$  beam incident on the  $\text{NaCl}$  target. The  $\text{Li}^6$  reaction is

then at least 750 times stronger than the  $\text{Li}^7$  reaction. This may be the result of the low reaction energy along with the general inhibition of  $\text{Li}^7$  reactions noted earlier.

### CONCLUSIONS

Considering all these reactions together, one could say that the general characteristics of lithium beam reactions below 4 Mev are:

- (a) A small increase in energy always results in a large increase in yield.
- (b) The reaction rate goes down rapidly as the nuclear charge of the target is increased.
- (c) The yield will be low when a large amount of nuclear material is transferred between the beam and target nuclei, and will be considerably larger when a smaller amount is transferred. A  $(\text{Li}^6, \text{Li}^5)$  reaction, for example, will be much more prolific than the  $(\text{Li}^6, n)$  reaction with the same target.
- (d) There is some indication that  $\text{Li}^6$  reactions are somewhat more prolific than  $\text{Li}^7$  reactions.

### ACKNOWLEDGMENTS

The author would like to express his thanks to Donald G. Seal for assembling the low-background beta-counter apparatus, to Stanley J. Brodsky who assisted with the calculations, and to the many others who gave valuable assistance in carrying out this work.

## $\text{Al}^{27}(n, \alpha)\text{Na}^{24}$ Cross Section as a Function of Neutron Energy

H. W. SCHMITT AND J. HALPERIN  
Oak Ridge National Laboratory, Oak Ridge, Tennessee  
(Received September 16, 1960)

The cross section for the  $\text{Al}^{27}(n, \alpha)\text{Na}^{24}$  reaction has been measured as a function of neutron energy in the range  $6.1 \leq E_n \leq 8.3$  Mev and at 14.8 Mev. Measurements were made relative to the fission cross section of  $\text{U}^{238}$ ; activation techniques were used to determine the number of  $\text{Al}^{27}(n, \alpha)$  events. While a number of peaks and valleys appear in the cross section versus energy curve, there is a general increase in cross section with increasing energy consistent with the Coulomb penetrability of the alpha particle.

### INTRODUCTION AND METHOD

THE  $\text{Al}^{27}(n, \alpha)\text{Na}^{24}$  reaction is of interest in the study of neutron interactions in intermediate nuclei. In addition, it is of practical importance in reactor technology, inasmuch as it is a threshold reaction which is suitable and convenient in certain circumstances, for high-energy neutron flux monitoring. This paper reports a measurement of the  $\text{Al}^{27}(n, \alpha)\text{Na}^{24}$  cross section as a function of neutron energy, relative to the known<sup>1</sup> fission cross section of  $\text{U}^{238}$ .

<sup>1</sup> W. D. Allen and R. L. Henkel, *Progress in Nuclear Energy* (Pergamon Press, New York, 1958), Vol. 2, Series 1. Cross-section values were taken from the smooth curve of Fig. 30.

The  $Q$  value for the reaction is  $-3.136$  Mev,<sup>2</sup> although, as will be seen, the cross section increases to values of the order of a few millibarns only at a neutron energy of about 6 Mev.

The experimental arrangement used in these measurements is shown schematically in Fig. 1. Monoenergetic neutrons were obtained from the  $\text{D}(d, n)\text{He}^3$  reaction using the ORNL 5.5-Mv Van de Graaff generator. Neutrons in a small cone about  $0^\circ$  with respect to the charged-particle beam were incident on an aluminum metal sample and on a thin deposit of

<sup>2</sup> P. M. Endt and C. M. Braams, *Revs. Modern Phys.* **29**, 683 (1957).

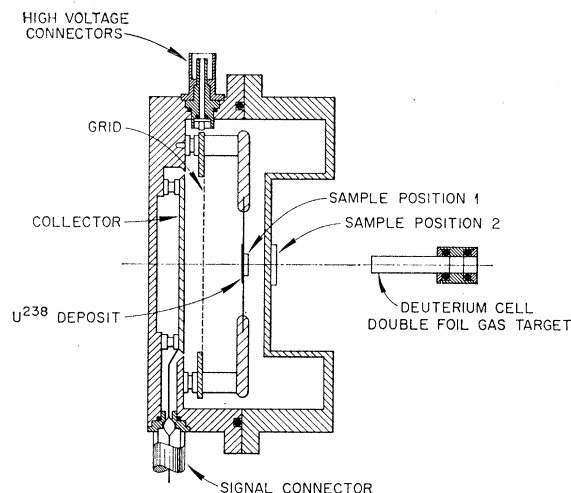


FIG. 1. Experimental arrangement for measurement of the  $\text{Al}^{27}(n, \alpha)\text{Na}^{24}$  cross section. Aluminum samples were placed in position 1 for experiments 1 and 2, and in position 2 for experiment 3.

$\text{U}^{238}$  as shown in the figure; the neutron energy was varied by changing the incident deuteron energy. The aluminum sample was located at position 1 to reduce geometric corrections for absolute cross section measurements; position 2, convenient for rapid sample changes, was used for detailed excitation function determinations.

The number of  $\text{Al}^{27}(n, \alpha)\text{Na}^{24}$  reactions occurring during an irradiation was obtained from a subsequent measurement of the gamma activity in the sample due to  $\text{Na}^{24}$  (half-life = 15.0 hr). A  $1\frac{1}{2}$  in.  $\times$  2 in. well-type scintillation crystal was used to count the 2.75- and 1.37-Mev gamma rays from the  $\text{Na}^{24}$  decay. Calibration was accomplished by comparison with a standard  $4\pi$  gamma-ray detector, calibrated in turn relative to absolute  $4\pi$  beta counting measurements. Except for the initial activity (9.5-min half-life) due to  $\text{Mg}^{27}$  formed from the  $\text{Al}^{27}(n, p)\text{Mg}^{27}$  reaction, only the characteristic 15.0-hour decay of  $\text{Na}^{24}$  was observed.

Fragments from the neutron-induced fission of  $\text{U}^{238}$  were counted in  $2\pi$  geometry in the thin-walled gridded ionization chamber shown schematically in Fig. 1. The two  $\text{U}^{238}$  samples used during the course of these measurements were electroplated in the form of  $\text{U}_3\text{O}_8$  onto 0.010-inch-thick platinum backings. Masses of the fissile deposits were determined by alpha-particle counting. Pulse-height spectra of alpha particles from the  $\text{U}^{238}$  deposits, counted in the ionization chamber of Fig. 1, were obtained; the absolute rate of alpha particle emission from each deposit was thus determined. In obtaining the mass of a deposit, corrections were included for the backscattering of alpha particles (counting geometry factor = 0.52)<sup>3</sup> and for finite deposit

thickness. The  $\text{U}^{238}$  half-life was assumed to be  $(4.51 \pm 0.02) \times 10^9$  years.<sup>4</sup> The deposits contained fissionable impurities to an extent less than one part in  $10^5$ .

Fission counts were recorded using duplicate amplifiers and scalars. Fission events were identified as counts above the integral pulse-height discriminator levels in the standard pulse amplifiers; the discriminator biases were set to reject alpha particle counts and other backgrounds not associated with neutron irradiation. A small fraction of the fragments (those emitted almost tangential to the deposit surface) lost sufficient energy in the deposit to give pulses below the discriminator bias setting. The correction for these fragments, determined from integral bias curves, amounted to 2 to 3% with an estimated uncertainty of 1%.

Background counts throughout the present experiment were measured under conditions and settings identical to those of the neutron irradiations, except that the target gas (tritium or deuterium) was replaced with helium. Backgrounds in fission counting ranged from one percent or less at the lowest deuteron energies to about 6% at the highest deuteron energy; the corresponding backgrounds in aluminum activity were less than one percent in all cases.

Neutron energies were determined by means of standard methods; published tables<sup>5</sup> were used to relate incident deuteron energy to neutron energy. Account was taken of deuteron energy loss in the thin nickel foils, in the helium gas used for cooling, and in the mean thickness of deuterium. Deuteron currents up to 15 microamperes were used in the double foil gas target.<sup>6</sup> The foil thicknesses were measured by accelerating protons onto the assembled target with a small amount of tritium in the gas cell and measuring the incident deuteron energy corresponding to the  $\text{T}(p, n)\text{He}^3$  reaction threshold energy. The thicknesses of all foils were also measured with a  $\text{C}^{14}$  beta-ray "thickness gauge;" on those occasions when a target foil was broken it was replaced with one of the same thickness as determined from the beta-ray measurements.

The  $(n, \alpha)$  reaction cross section was obtained for each neutron energy from the following equation:

$$\sigma_{n, \alpha} = \sigma_f(E_n) \times \frac{n_\alpha}{n_f} \times \frac{\bar{\phi}(\text{U}^{238})}{\bar{\phi}(\text{Al})}, \quad (1)$$

where  $\sigma_f(E_n)$  represents the known<sup>1</sup> fission cross section of  $\text{U}^{238}$ ,  $n_\alpha$  represents the number of  $n, \alpha$  reactions per aluminum atom in the sample,  $n_f$  the number of  $\text{U}^{238}$  fission counts per atom of  $\text{U}^{238}$ , and  $\bar{\phi}(\text{U}^{238}$  or Al) the average neutron flux (neutrons/cm<sup>2</sup> sec) incident on the  $\text{U}^{238}$  or aluminum. The ratio  $\bar{\phi}(\text{U}^{238})/\bar{\phi}(\text{Al})$  was calculated from published angular distributions of source neutrons.<sup>5</sup> It is to be noted that the ratio

<sup>3</sup> J. A. Crawford, *The Transuranium Elements: Research Papers* (McGraw-Hill Book Company, Inc., New York, 1949), Paper No. 16.55, National Nuclear Energy Series, Plutonium Project Record, Vol. 14B, Div. IV.

<sup>4</sup> A. F. Kovarik and N. I. Adams, *Phys. Rev.* **98**, 46 (1955).

<sup>5</sup> J. L. Fowler and J. E. Brolley, Jr., *Revs. Modern Phys.* **28**, 103 (1956).

<sup>6</sup> R. W. Lamphere (to be published).

$\bar{\phi}(U^{238})/\bar{\phi}(Al)$ , applied to the present experiment, is different from unity principally because of the difference in diameter of the aluminum and uranium samples; it is, however, relatively insensitive to the neutron angular distribution and hence to neutron energy.

A measurement at 14.8 Mev was carried out using the ORNL Cockcroft-Walton accelerator. Deuterons were accelerated to an energy of 190 keV and were incident on a conventional solid water-cooled Zr-T target. The target holder was specially constructed so that only a 0.040-inch thickness of water intervened between the neutron source and the chamber. Samples were located at position 1 in the chamber, Fig. 1. Four separate runs were made using two different U<sup>238</sup> deposits; the results were in excellent agreement. Procedures and considerations similar to those described above were applied in these measurements.

### RESULTS AND DISCUSSION

The cross-section results obtained from these measurements are given in Fig. 2 and Table I. In experiments 1 and 2 the samples were located in position 1 (see Fig. 1), and absolute values of the cross section were obtained. Experiment No. 3 was designed for convenient change of aluminum samples, i.e., sample position 2 was used, so that the shape of the cross section versus energy curve could be readily obtained in detail. Cross-section values obtained from experiment No. 3

TABLE I. Final results of present experiment, taken from a smooth curve drawn through the original data points. Energies of maxima and minima are indicated by asterisks. Entries in column 3 are taken from reference 1.

Neutron energy (Mev)	$\sigma_{n,\alpha}(Al)/\sigma_f(U^{238})$	$\sigma_f(U^{238})$ (barns)	$\sigma_{n,\alpha}(Al)$ (millibarns)
6.10	0.0029	0.648	(1.9)
6.20	0.0037	0.682	(2.5)
6.30	0.0050	0.722	(3.6)
6.40	0.0056	0.766	(4.3)
6.50	0.0072	0.810	5.8
6.60	0.0097	0.845	8.2
6.66*	0.0109	0.863	9.4
6.70	0.0095	0.876	8.3
6.73*	0.0090	0.884	8.0
6.80	0.0119	0.902	10.7
6.90	0.0163	0.928	15.1
7.00	0.0179	0.950	17.0
7.10	0.0193	0.964	18.6
7.20	0.0224	0.976	21.9
7.27*	0.0245	0.982	24.1
7.30	0.0235	0.985	23.1
7.37*	0.0211	0.991	20.9
7.40	0.0215	0.993	21.3
7.50	0.0256	1.00	25.6
7.60	0.0310	1.005	31.2
7.70*	0.0343	1.01	34.6
7.80*	0.0315	1.01	31.8
7.90	0.0340	1.01	34.3
8.00	0.0415	1.01	41.9
8.10*	0.0489	1.01	49.4
8.20	0.0439	1.01	44.3
8.24*	0.0431	1.01	43.5
8.30	0.0450	1.01	45.5
14.76	0.0943	1.24	117.0

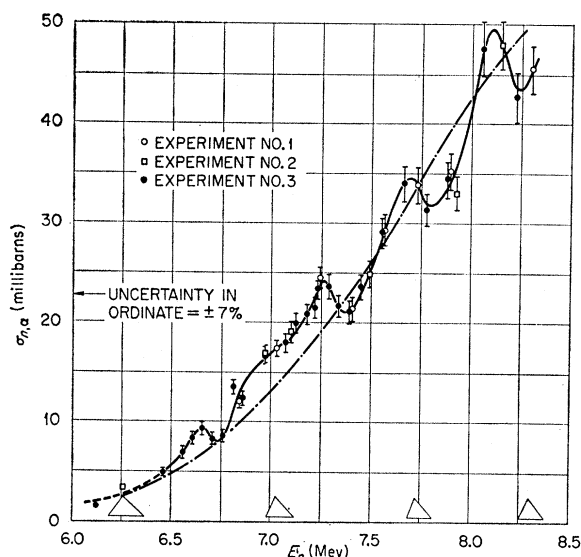


FIG. 2. Al<sup>27</sup>(n, α)Na<sup>24</sup> cross section as a function of neutron energy. Bases of the triangles indicate total neutron energy spread, including effects of energy degradation of deuterons in the target and of angular spread of the sample. Error flags indicate combined statistical and other point-to-point uncertainties; uncertainty in absolute value is  $\pm 7\%$  as indicated. The broken curve shows the results of calculations described in the text.

are therefore normalized to the absolute values obtained in experiments 1 and 2. Uncertainties arising from counting statistics, background determinations, and other point-to-point effects, are indicated by error flags in Fig. 2. Systematic uncertainties, e.g., in the U<sup>238</sup> masses or in the absolute value of  $\sigma_f$ , combine to give an absolute uncertainty in  $\sigma_{n,\alpha}(Al)$  of  $\pm 7\%$ . Because of the large number of data points, the values tabulated in Table I are those taken from a smooth curve representing the best visual fit to the data. The measured quantity is  $\sigma_{n,\alpha}(Al)/\sigma_f(U^{238})$ ; values used for  $\sigma_f(U^{238})$  are also tabulated, together with the resulting values of  $\sigma_{n,\alpha}(Al)$ .

Measurements of the Al<sup>27</sup>(n, α)Na<sup>24</sup> cross section at a neutron energy of 14.76 Mev yielded a cross section value of  $117 \pm 8$  millibarns. This value is the weighted mean of the results of four experiments as described in the preceding section. Individual values were 116 mb, 116 mb, 117 mb, and 118 mb. The mean value of  $117 \pm 8$  mb, where the uncertainty includes all statistical and systematic uncertainties, is in excellent agreement with that obtained by Kern *et al.*<sup>7</sup> at this energy and is consistent with those values obtained by Grundl *et al.*,<sup>8</sup> Khurana and Hans,<sup>9</sup> and Yasumi.<sup>10</sup> The present result appears to be inconsistent with measurements in

<sup>7</sup> B. D. Kern, W. E. Thompson, and J. M. Ferguson, *Nuclear Phys.* **10**, 226 (1959).

<sup>8</sup> J. A. Grundl, R. L. Henkel, and B. L. Perkins, *Phys. Rev.* **109**, 425 (1958).

<sup>9</sup> C. S. Khurana and H. S. Hans, *Nuclear Phys.* **13**, 88 (1959).

<sup>10</sup> S. Yasumi, *J. Phys. Soc. Japan* **12**, 443 (1957).

this energy region by Forbes<sup>11</sup> and by Paul and Clarke.<sup>12</sup> The cross section versus energy curve of Fig. 2 is generally consistent with values obtained by Grundl *et al.*<sup>8</sup> for three neutron energies up to 8.1 Mev. The present results are inconsistent, however, with earlier Los Alamos data (cited in reference 8) giving the shape of the cross section versus neutron energy curve for energies below about 7.5 Mev.

Calculations have been made of the shape of the  $\text{Al}^{27}(n,\alpha)\text{Na}^{24}$  cross section as a function of incident neutron energy above threshold. The continuum theory has been used together with certain simplifying assumptions. In this treatment the cross section is written

$$\sigma(n,\alpha) = \sigma_{cn} G_c(\alpha), \quad (2)$$

where  $\sigma_{cn}$  is the neutron cross section for compound nucleus formation, and  $G_c(\alpha)$  is the probability of decay of the compound nucleus by alpha-particle emission. On the basis of a statistical approach,<sup>13</sup> in which, however, angular momentum effects are neglected,  $G_c(\alpha)$  can be written

$$G_c(\alpha) = \frac{\int_0^{\epsilon_n+Q} \sigma_{c\alpha}(\epsilon_\alpha) k_\alpha^2 \rho_B(\epsilon) d\epsilon_\alpha}{\int_0^{\epsilon_n} \sigma_{cn}(\epsilon_n) k_n^2 \rho_A(\epsilon) d\epsilon_n}, \quad (3)$$

where  $\sigma_{c\alpha}(\epsilon_\alpha)$  and  $\sigma_{cn}(\epsilon_n)$  are the compound nucleus formation cross sections, respectively, for an alpha particle of center-of-mass energy  $\epsilon_\alpha$  and for a neutron of center-of-mass energy  $\epsilon_n$ ; the compound nucleus is the same in both cases, i.e.,  $\text{Al}^{28*}$ . In Eq. (3)  $k_\alpha$  and  $k_n$  are the alpha-particle and neutron wave numbers, and  $\rho_A(\epsilon)$  and  $\rho_B(\epsilon)$  are the densities of states in the target nucleus  $A$  and residual nucleus  $B$ . The particle energies are related by  $\epsilon_\alpha = \epsilon_n + Q$ .

Since there are relatively few states in the region of interest in  $\text{Na}^{24}$ , the approximation  $\rho_B = \text{constant}$  was made for the present limited energy range. For the case of  $\text{Al}^{27}$ , the level density  $\rho_A(\epsilon)$  was assumed to follow the statistical relation  $\rho_B(\epsilon) \propto \exp[2(a\epsilon)^{1/2}]$ , with  $a = 0.5 \text{ Mev}^{-1}$ .<sup>14</sup> The cross section for formation of the compound nucleus by neutrons was taken from con-

tinuum theory estimates,<sup>14</sup> while the compound nucleus formation cross section for alpha particles were taken from the optical model calculations of Igo.<sup>15</sup>

Results of the calculations are shown in Fig. 2. The agreement of the calculations with experiment is considered satisfactory in view of the approximate nature of the calculations; also the measured  $\text{Al}^{27}(n,\alpha)$  cross section reaches a peak in the neutron energy range 9–12 Mev, based on present data together with the decreasing cross section found by Kern *et al.*<sup>7</sup> in the 12–16 Mev energy range. Competition with other reactions, particularly the  $(n,2n)$ ,  $(n,d)$ , and  $(n,t)$  reactions, should, of course, become important in the higher energy range.

Concerning the structure in the measured  $\text{Al}^{27}(n,\alpha)\text{Na}^{24}$  cross-section curve, Wildermuth<sup>16</sup> has suggested that this may be a consequence of nuclear behavior according to the cluster model. Thus, if the compound nucleus prior to decay by alpha-particle emission can assume the form of an alpha-particle cluster moving around a  $\text{Na}^{24}$  nucleus, then this system will have resonances whose average widths and spacings may be estimated from cluster-model considerations. Because of the poor neutron resolution (relative to the widths of peaks in the measured cross-section curve) in the present experiment, the separation of these "levels" provides the more sensitive test. While the cluster model as applied to such reactions has not yet reached a fully-developed quantitative form, it may be significant that for the present case Wildermuth<sup>16</sup> has estimated a separation of the order of magnitude of 400 kev or more, a result not inconsistent with the present experimental results. It is suggested that a systematic investigation of  $(n,\alpha)$  cross sections and angular distributions as a function of atomic weight of the target nucleus and incident neutron energy may be quite fruitful from the point of view of the cluster model. Of most interest<sup>16</sup> would be those cases for which the  $(n,\alpha)$  cross section for  $\alpha$  decay to a specific state in the residual nucleus can be measured. Similar experiments for other clusters in the outgoing channel may also lead to results analogous to those found here.

#### ACKNOWLEDGMENT

The authors gratefully acknowledge the assistance of R. E. Druschel in measurements of some of the sample activities. Helpful discussions with G. R. Satchler and K. Wildermuth are gratefully acknowledged.

<sup>11</sup> S. G. Forbes, *Phys. Rev.* **88**, 1309 (1952).

<sup>12</sup> E. B. Paul and R. L. Clarke, *Can. J. Phys.* **31**, 267 (1955).

<sup>13</sup> See, for example, A. C. Douglas and N. MacDonald, *Nuclear Phys.* **13**, 382 (1959).

<sup>14</sup> See, for example, J. M. Blatt and V. F. Weisskopf, *Theoretical Nuclear Physics* (John Wiley & Sons, Inc., New York, 1952).

<sup>15</sup> G. Igo, *Phys. Rev.* **115**, 1665 (1959).

<sup>16</sup> K. Wildermuth (private communication, 1960).